Journal of Materials Chemistry A

RSC Publishing

PAPER

View Article Online
View Journal | View Issue

Ultrathin rechargeable all-solid-state batteries based on monolayer graphene†

Cite this: *J. Mater. Chem. A*, 2013, **1**, 3177

Di Wei,*[a] Samiul Haque,[a] Piers Andrew,[a] Jani Kivioja,[a] Tapani Ryhänen,[a] Amaia Pesquera,[b] Alba Centeno,[b] Beatriz Alonso,[b] Andrey Chuvilin[cd] and Amaia Zurutuza[b]

Received 21st November 2012
Accepted 9th January 2013

DOI: 10.1039/c3ta01183f

www.rsc.org/MaterialsA

The energy and power requirements of portable electronic devices and electric vehicles are ever increasing, driving research into novel battery structures with increased volumetric energy and power densities. Existing energy storage technologies cannot satisfy both of these requirements. There are many reports on the application of graphene in batteries and supercapacitors with enhanced power and energy densities; however, few results were shown on the performance of an electrochemical energy storage device made of monolayer graphene. The energy storage capability of monolayer graphene is investigated in this paper and it can contribute an understanding of the application of graphene materials in high energy and power density batteries. In parallel, flexible solid-state batteries will relax design constraints, giving the freedom to create new device form factors. A mechanically flexible all-solid state battery can be made of monolayer graphene grown by chemical vapour deposition (CVD) directly onto copper (Cu) foil. The total thickness of the resulting battery was ~50 μm. Such an ultrathin battery showed the highest energy density of 10 W h L^{-1} and the highest power density of 300 W L^{-1}. It also shows excellent cyclic stability and sustains a discharge current density of 100 μA cm^{-2} over 100 cycles, maintaining energy capacity over 0.02 mA h cm^{-2}.

1 Introduction

Graphite is the current industry standard material for lithium battery electrodes due to its reliability and effective lithium ion intercalation properties. Two-dimensional graphene is the basic component in all different graphitic forms of materials ranging from the three-dimensional graphite, one-dimensional carbon nanotubes to zero-dimensional fullerenes. Carbon nanotubes and other carbon nanomaterials had been utilized as novel electrode materials to enhance battery capacity and flexible form factors.[1] However, unmodified carbon nanotubes are not ideal candidate materials to be dispersed in either organic or aqueous solutions for wet-processing methods such as printing or spin-coating. Graphene-based materials are intriguing from the perspectives of both fundamental science and technology, because they can be easily formulated as ink, are chemically and thermally tolerant, electrically conductive and mechanically robust. Graphene has superior electrical conductivity to graphitic carbon, a high specific surface area of over 2600 $m^2 g^{-1}$,[2] and a broad electrochemical window that would be very advantageous for application in energy storage devices. Graphene sheets can be used as electrode materials with high rate capability and large capacity for rechargeable lithium secondary batteries due to their large reversible Li storage ability.[2–6] Studies of lithium storage and the use of graphene as a high-performance battery electrode have been carried out.[7,8] It is feasible to make electrochemical energy devices with both high energy and power density that can also work at high frequencies by using graphene.[9,10] Few-layer, nitrogen-doped graphene was used as a battery electrode and its rate capability was studied for current densities ranging from 1 μA cm^{-2} to 100 μA cm^{-1}.[4] The nominal capacity (~0.06 mA h cm^{-2}) was obtained for a discharge rate of 1 μA cm^{-2}.

To produce graphene, many methods have already been developed.[11–13] In 2004, Geim and co-workers[12] first reported graphene sheets prepared by micromechanical exfoliation (repeated peeling) of highly oriented pyrolytic graphite (HOPG). This scotch-tape method produces graphene with excellent material properties and hence is still widely used in many laboratories to obtain pristine graphene flakes for basic scientific research and for making proof-of-concept devices. The process is, however, not suitable for volume production and the flake size is limited to the micrometer range. Graphene can also be prepared by thermal decomposition of a SiC wafer under ultrahigh vacuum conditions[14] but the resulting graphene is

[a]Nokia Research Center, Broers Building, 21 J. J. Thomson Avenue, CB3 0FA, Cambridge, UK. E-mail: di.wei@nokia.com
[b]Graphenea S.A., Tolosa Hiribidea 76, 20018 Donostia-San Sebastián, Spain
[c]CIC nanoGUNE, Tolosa Hiribidea 76, 20018 Donostia-San Sebastián, Spain
[d]IKERBASQUE, Basque Foundation for Science, E-48011, Bilbao, Spain

† Electronic supplementary information (ESI) available: TEM and electrochemical characterization of a monolayer graphene battery. See DOI: 10.1039/c3ta01183f

composed of submicrometer-sized domains, which are not spatially uniform in size or number density over larger length scales. Chemical Vapour Deposition (CVD) is a popular technique to grow graphene on metal substrates.[13] CVD has the potential to enable large scale graphene production for electronic applications such as thin film transistors, solar cells and touch panels which require large area graphene sheets of the order of tens of centimeters in size. Using this process, graphene may be subsequently transferred to a separate substrate. Alternative cost-effective ways of graphene synthesis using solution-based processes are *via* chemical reduction of graphene oxide (GO)[11] or liquid phase exfoliation starting from graphite.[15] These methods offer the scope to produce large quantities of graphene economically to the expense of a considerable decrease in graphene quality/properties. In particular, chemical reduction of GO is a simple process and sheets as large as 50 micrometers have been made, and they can then be subsequently chemically modified. Within the family of chemical methods, the recently developed process of electrochemical exfoliation is regarded as a green method that allows easy tunability of the obtained products by variation of the applied potential.[16–18] Chemical reduction of graphene oxide has been a cost-effective method of synthesis of graphene electrodes for Li batteries[5] but many defects are created during the reaction and these defects increase sheet resistance, reducing the open circuit voltage of the battery. It is also harder to control the number of layers deposited than it is with the CVD method. In this paper, graphene monolayer films were grown on Cu foil using CVD and their application as a battery electrode was studied, demonstrating important advantages for flexible batteries.

2 Results and discussion

Monolayer graphene grown on Cu foil, forming a combined electrode and current collector with a thickness of 25 μm, is shown in Fig. 1a. This cathode, together with a lithium foil anode of thickness 20 μm, was used to sandwich a thin solid polymer electrolyte, forming a cell with a total thickness of the order of 50 μm. The polymer electrolyte is composed of a high molecular weight poly(ethylene glycol) borate ester. The Lewis acid centers of the borate esters interact with the anion of the lithium salt resulting in enhanced lithium ion transport and the resulting performance of such polymer electrolytes is comparable with conventional liquid organic electrolytes at room temperature.[19] The packaged monolayer graphene battery is depicted in flexed states in Fig. 1b and c. To demonstrate the current delivery capability of the ultrathin battery, an LED was driven by the battery as shown in Fig. 1d. When conventional lithium ion batteries are mechanically bent or twisted, the dried slurry cathode coatings will crack and can even fall away from the charge collector foil. This will cause the battery to fail and limit its use in flexible electronic applications. In our experiment, it is demonstrated that even a monolayer of graphene works as an excellent battery electrode with extraordinary mechanical flexibility with a bending radius of less than 1 mm and ultrathin thickness.

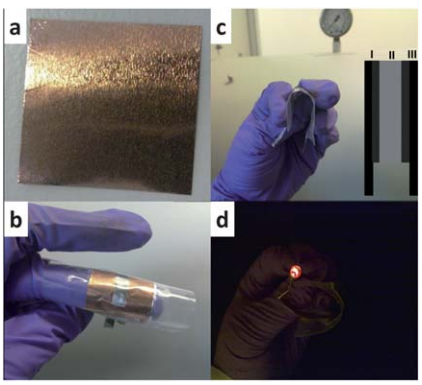

Fig. 1 Pictures of (a) monolayer graphene grown on Cu; (b and c) flexible graphene battery undergoing deformation, inset in (c) shows the sandwich structure of the battery: (I) graphene on Cu foil as a cathode, (II) polymer electrolyte, and (III) lithium foil as an anode; (d) graphene monolayer battery powering a Light Emitting-Diode (LED), demonstrating the ability to deliver ~mA current.

In many applications, CVD-grown graphene is generally transferred from Cu to a more appropriate substrate and the transfer process may lead to a degradation of the excellent material properties. For energy storage applications, Cu foil is one of the mostly used charge collecting substrates, so transfer is not necessary and the graphene material properties are preserved. To assess the quality and uniformity of the graphene used in the battery electrodes, Raman spectroscopy and transmission electron microscopy (TEM) techniques were employed. The Raman spectrum of graphene is composed of three major peaks: the D-, G- and 2D-bands. The D-band, centered at ~1328 cm^{-1}, is attributed to disorder-induced first-order scattering (interlayer effects), whilst the G-band at ~1583 cm^{-1} is a result of in-plane (intralayer) vibrations of the sp^2-hybridized carbon atoms and the 2D-band located around ~2700 cm^{-1} is an overtone of the D-band and can be attributed to a two phonon double resonance Raman process.[20] Based on these characteristic peak positions and relative intensities together with the optical colour contrast of the deposited graphene on a substrate, information about the number of layers and the quality of the graphene can be inferred. Raman characterization of the graphene grown on Cu foil was carried out after transfer to a 300 nm thick silicon dioxide layer on top of a silicon wafer using a wet chemical etching process. High quality micromechanically exfoliated monolayer graphene samples exhibit Raman spectra with a single Lorentzian line shape 2D peak, no D peak and, as a result, the D/G peak ratio is zero, implying that the sample is pristine and has no defects. Fig. 2(i) shows the spectrum of a micromechanically exfoliated graphene sample and this was used as a benchmark for assessing the quality of the CVD graphene. A laser of wavelength 457 nm was used to carry out Raman spectroscopy at three different locations on the CVD graphene sample: center (ii), bottom right (iii) and top left (iv), and the quality as well as the uniformity of the sample was determined. The first comparison was made by investigating the shape of the 2D peak and it was noted that for all the spectra (ii, iii and iv) the shape matched that observed for exfoliated monolayer graphene (Fig. 2(i)).[20] The three traces showed a

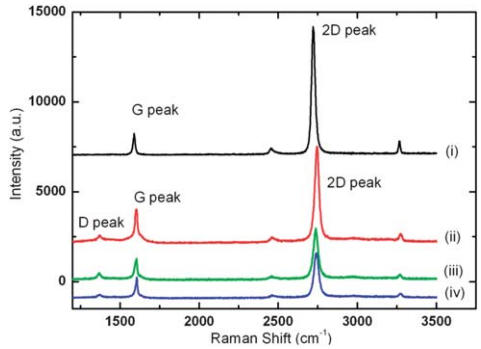

Fig. 2 Raman spectra taken from (i) micromechanically exfoliated monolayer graphene, (ii) centre of the CVD graphene, (iii) bottom right area of the CVD graphene and (iv) top left area of the CVD graphene.

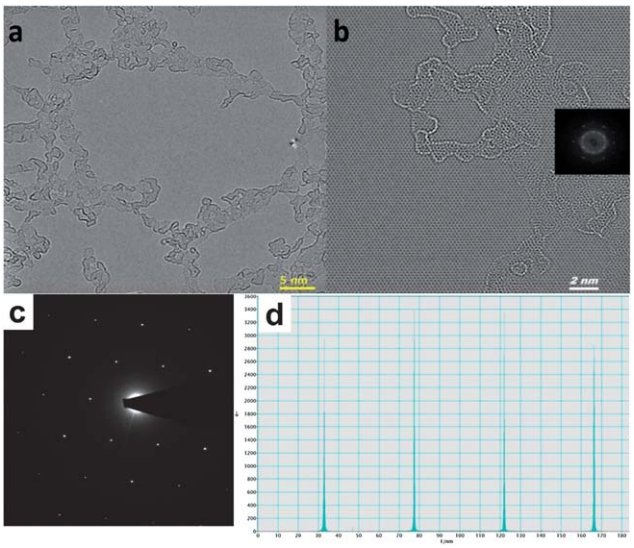

Fig. 3 (a) TEM overview image of the monolayer graphene film membrane and (b) high resolution TEM image of the monolayer graphene film membrane. Inset: FFT pattern of the monolayer graphene. (c) Selected area electron diffraction (SAED) pattern of the monolayer graphene membrane. (d) Line scan through the reflections.

single Lorentzian peak around ~2700 cm^{-1}, therefore it can be established that the film was composed of high quality monolayer graphene. The sample was uniform over a large area of the substrate and very low spectral intensity D peaks were observed so it can be deduced that the monolayer graphene had very few or negligible defects.

In some instances, Raman spectroscopy is not completely conclusive in determining the number of graphene layers. In the case of AB Bernal stacked bilayer graphene the Raman spectra is conclusive in distinguishing mono- and bi-layer graphene.[20] The main feature that distinguishes monolayer from AB Bernal stacked bilayer graphene is the line shape of the 2D peak where in the latter case peak splitting occurs and it is not single Lorentzian anymore. As a consequence, the Raman signature for mono and AB Bernal stacked bilayer graphene is quite distinctive.[20] On the other hand, non-AB Bernal stacked bilayer graphene has very similar Raman spectra to that of monolayer graphene[21] due to the lack of or weak coupling between the layers. The line shape of the 2D peak can be fitted with a single Lorentzian curve in both cases. Therefore, the use of a complementary characterization technique is highly recommended. TEM allows the clear distinction between mono-, bi- and few-layer graphene[22,23] as well as providing the potential to determine the different grain orientations within monolayer graphene grown *via* CVD.[24] In addition, the stacking order between the layers in the case of bilayer graphene (AB and non-AB Bernal stacked, orientated *vs.* twisted) can also be determined using this technique.

The analysis of the electron diffraction or Fast Fourier Transform (FFT) patterns of the high resolution TEM images enables the determination of the number of layers and the rotation between the layers; in addition, diffraction allows the unambiguous differentiation of a monolayer from multilayer graphene (in the case where there is more than one layer present).[22,23] High resolution TEM provides images of individual atoms as well as atomic structure of topological defects.

The monolayer suspended graphene film shown in Fig. 3a and b is quite uniform and free from defects over relatively large areas and the hexagonal honeycomb structure of the monolayer graphene can be clearly observed. However, completely contamination free graphene samples are practically not possible to obtain and the presence of some contamination can be detected.[23] The contamination is mainly composed of some organic residuals and a trace amount of Cu from transfer of graphene from the Cu substrate to the TEM grid for the TEM measurement. The images also show atomic resolution of the graphene honeycomb lattice where single carbon atoms can be observed either as white (Fig. 3a) or black spots (Fig. 3b). Large areas that are completely free from adsorbents can be observed. The analysis of the Fast Fourier Transform pattern of the monolayer graphene film shown in the inset of Fig. 3b indicates that the film is a monolayer since there is a single set of hexagonal ring patterns. Please note that in this image the contrast is reversed, *i.e.* carbon atoms appear as dark spots. Furthermore, it can be concluded that we do not have non-AB Bernal stacked or twisted bilayer graphene, in which case the high resolution TEM image would have shown a Moire pattern structure as well as two sets of hexagonal rings in the FFT pattern. A selected area electron diffraction (SAED) pattern was acquired from an approximate 100 nm sized area (Fig. 3c) and the intensity profile through the reflections was measured (see Fig. 3d). Again, a single set of hexagonal rings were observed, indicating the absence of non-interacting bilayer or multilayer graphene where two or more sets of hexagonal rings would have been present. In the case of non-AB Bernal stacked bilayer graphene the diffraction intensities of the second order reflections would be roughly twice that of the inner peaks. For monolayer graphene the first and second order peaks are roughly equal as it is in our case (Fig. 3d). The combination of both Raman spectroscopy and the results obtained from the intensity profile from FFT-TEM indicated that the graphene grown on the Cu foil is indeed monolayer. The electrochemical process of lithium intercalation into the graphene monolayer was studied by cyclic voltammetry and the voltammograms are shown in the ESI.†

To demonstrate the flexible nature of the graphene monolayer battery, pouch cells (Fig. 1) were packaged using a Fuji impulse V300 vacuum sealer. However, to make standardized comparisons with ref. 4, 2032 coin cells were also assembled inside an mBraun glove box (H_2O < 0.1 ppm, O_2 < 0.1 ppm). In such batteries, lithium foil was used as the anode with a polymer electrolyte composed of a high molecular weight poly(ethylene glycol) borate ester as described before. The assembled coin cells were analyzed using a Maccor battery tester. In most references reporting batteries based on graphene, the current densities are chosen in the range of 1 μA cm^{-2} to 100 μA cm^{-1}.[4] As integrated circuits are reduced in size, despite the lower current demanded by smaller devices, there is a trend toward higher current densities to achieve higher device numbers in ever smaller chip areas. Thus a battery that can provide a higher current density is needed. In this paper, our battery was tested at various current densities from 100 μA cm^{-2}, 300 μA cm^{-2}, up to 600 μA cm^{-2}, which is the highest discharge current density reported for monolayer graphene batteries.

Fig. 4a shows the voltage *versus* specific capacity plots conducted at a current density of 100 μA cm^{-2}. The first discharge curve shows a shoulder at about 0.6 V. This discharge plateau can be attributed to the formation of a solid electrolyte interface (SEI) layer on the graphene which is associated with electrolyte decomposition and the formation of an organic lithium compound.[4] At a discharge current density of 100 μA cm^{-2}, the energy capacity decreased from the initial energy capacity of 0.06 mA h cm^{-2} to a capacity of ~0.02 mA h cm^{-2}, which was maintained and was stable even after 100 cycles. At higher discharge current densities of 300 μA cm^{-2} and even 600 μA cm^{-2}, the energy capacity decreased further, but a retention of about 50% at a current density of 300 μA cm^{-2} was observed as shown in Fig. 4b. Fig. 4c shows the modeled equivalent circuit of electrochemical impedance spectroscopy (EIS), where R_Ω stands for the electrolyte resistance, R_{CT} the charge transfer resistance, and Z_w the 'Warburg' element related to the Li ion diffusion. More specifically, the electrolyte resistance (R_Ω) of our monolayer graphene battery is very low, which is only about 6 Ohm. R_{CT} involves resistance from Li ion migration through the surface film and interfacial charge transfer and Z_w accounts for the Li ion diffusion in graphene. The impedance spectrum clearly reflects the serial, multistep nature of the Li insertion–deintercalation process. By fitting the impedance response with a proper equivalent circuit as shown in the inset of Fig. 4c, one can refine the analysis to show that at high-to-medium frequencies, the large semi-circle indicates charge transfer resistance (R_{CT}), which includes Li migration within the film surface coupled with film capacitance, SEI formation and resistance of charge transfer. The total charge transfer resistance of our graphene battery is about 68 Ohm, which is similar to the R_{CT} of high performance batteries based on carbon nanotubes[25] and graphene thin films.[26] At lower frequencies, the impedance spectrum contains a potential dependent Warburg element (Z_w) that is related to the solid state diffusion of lithium ions into graphene. The Ragone plot in Fig. 4d was calculated based on the volume of a whole cell. For the monolayer graphene battery, an energy density of 10 W h L^{-1} can be obtained at a power density of 50 W L^{-1}. Such energy density is much higher than the highest energy density of graphene supercapacitors (~1 W h L^{-1})[27] and similar to Li thin film batteries but the power density of a lithium thin film battery can only reach 5 W L^{-1}, as compared in ref. 27. A power density of 300 W L^{-1} can be obtained at an energy density of 2.5 W h L^{-1}. It can be seen that our electrochemical device based on monolayer graphene behaves like a hybrid supercapacitor and battery. This is also in accordance with previous reports on the high energy and power density batteries made of graphene flakes.[9,10] Rapid surface Li^+ absorption and ultrafast Li^+ diffusion and electron transport makes this material superior to the conventional bulk electrode materials based on Li intercalation and conversion reactions. It should be noticed that the battery response is purely from the monolayer graphene on the Cu substrate, because when using pure Cu foil without graphene as an electrode in the same structure there is no electrochemical response at all and the open circuit voltage is zero.

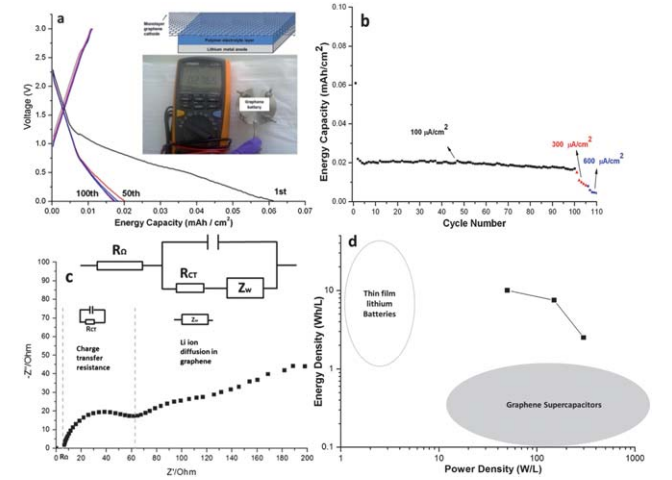

Fig. 4 Electrical characterization of the monolayer graphene battery (a) discharge and charge voltage profiles for cycling at current density of 100 μA cm^{-2}, (b) rate capability study, showing discharge energy capacity *vs.* cycle number for various current densities (100 μA cm^{-2} for the first 100 cycles, then 300 μA cm^{-2} for 5 cycles and 600 μA cm^{-2} for the final 5 cycles), (c) Nyquist plot of the battery response to a sinusoidal wave input with an amplitude of 5 mV in the frequency range from 100 kHz to 10 mHz and (d) volumetric Ragone plot based on the total volume of a monolayer graphene pouch cell battery. The energy and power density ranges of thin film lithium batteries and graphene supercapacitors in the Ragone plot are based on the data from ref. 27.

3 Conclusions

Direct fabrication of a graphene electrode on a metallic current collector substrate offers a strategy to produce a binder-free, robust, bendable and mechanically flexible battery. In this paper, we demonstrated that an ultrathin rechargeable all-solid-state battery based on a monolayer of graphene provides sufficient current to drive an LED with open circuit voltage over 2.5 V. The use of CVD grown graphene on Cu foil directly does not involve transfer of a substrate which is also a tedious and

costly way and can significantly contaminate the graphene layers easily. This paper also had a detailed study on the properties of monolayer graphene and its application in batteries, which will provide further understanding when using graphenes for high-power and high-energy density electrochemical energy storage devices. Coupling with CVD grown graphene directly to battery manufacturing may also enable a cost-effective roll-to-roll mass production process for future flexible batteries. The highly conductive property of graphene with its enormous active area may be able to impart special property as both a lithium ion conductor and an electronic conductor to reduce both the size and weight of the battery without sacrificing the energy capacity.

References

1 P. Victor, M. M. Shaijumon, A. Kumar, S. Murugesan, L. Ci, R. Vajtai, R. Linhardt, O. Nalamasu and P. M. Ajayan, Flexible Energy storage devices based on nanocomposite paper, *Proc. Natl. Acad. Sci. U. S. A.*, 2007, **104**, 13574.
2 S. M. Paek, E. J. Yoo and I. Honma, *Nano Lett.*, 2009, **9**, 72.
3 E. J. Yoo, J. Kim, E. Hosono, H. S. Zhou, T. Kudo and I. Honma, *Nano Lett.*, 2008, **8**, 2277.
4 A. L. M. Reddy, A. Srivastava, S. R. Gowda, H. Gullapalli, M. Dubey and P. M. Ajayan, *ACS Nano*, 2010, **4**, 6337.
5 D. Wei, P. Andrew, H. Yang, J. Jiang, W. Ruan, D. Han, L. Niu, C. Bower, T. Ryhanen, M. Rouvala, G. A. J. Amaratunga and A. Ivaska, *J. Mater. Chem.*, 2011, **21**, 9762.
6 Z. S. Wu, W. Ren, L. Xu, F. Li and H. M. Cheng, *ACS Nano*, 2011, **5**, 5463.
7 N. Li, Z. Chen, W. Ren, F. Li and H. M. Cheng, *Proc. Natl. Acad. Sci. U. S. A.*, 2012, **109**(43), 17360–17365.
8 X. Zhao, C. M. Hayner, M. C. Kung and H. H. Kung, *ACS Nano*, 2011, **5**(11), 8739–8749.
9 C. Liu, Z. Yu, D. Neff, A. Zhamu and B. Z. Jang, *Nano Lett.*, 2010, **10**, 4863.
10 B. Z. Jang, C. Liu, D. Neff, Z. Yu, M. C. Wang, W. Xiong and A. Zhamu, *Nano Lett.*, 2011, **11**, 3785–3791.
11 S. Park and R. S. Ruoff, *Nat. Nanotechnol.*, 2009, **4**, 217–224.
12 K. S. Novoselov, A. K. Geim, S. V. Morozov, D. Jiang, Y. Zhang, S. V. Dubonos, I. V. Grigorieva and A. A. Firsov, *Science*, 2004, **306**, 666–669.
13 X. S. Li, W. W. Cai, J. H. An, S. Kim, J. Nah, D. X. Yang, R. D. Piner, A. Velamakanni, I. Jung, E. Tutuc, S. K. Banerjee, L. Colombo and R. S. Ruoff, *Science*, 2009, **324**, 1312–1314.
14 K. V. Emtsev, A. Bostwick, K. Horn, J. Jobst, G. L. Kellogg, L. Ley, J. L. McChesney, T. Ohta, S. A. Reshanov, J. Rohrl, E. Rotenberg, A. K. Schmid, D. Waldmann, H. B. Weber and T. Seyller, *Nat. Mater.*, 2009, **8**, 203–207.
15 Y. Hernandez, V. Nicolosi, M. Lotya, F. M. Blighe, Z. Sun, S. De, I. T. McGovern, B. Holland, M. Byrne, Y. K. Gun'Ko, J. J. Boland, P. Niraj, G. Duesberg, S. Krishnamurthy, R. Goodhue, J. Hutchison, V. Scardaci, A. C. Ferrari and J. N. Coleman, *Nat. Nanotechnol.*, 2008, **3**, 563–568.
16 C. Y. Su, A. Y. Lu, Y. Xu, F. R. Chen, A. N. Khlobystov and L. J. Li, *ACS Nano*, 2011, **5**, 2332–2339.
17 J. Wang, K. K. Manga, Q. Bao and K. P. Loh, *J. Am. Chem. Soc.*, 2011, **133**, 8888–8891.
18 D. Wei, L. Grande, V. Chundi, R. White, C. Bower, P. Andrew and T. Ryhanen, *Chem. Commun.*, 2012, **48**, 1239–1241.
19 Y. Kato, K. Suwa, H. Ikuta, Y. Uchimoto, M. Wakihara, S. Yokoyama, T. Yabe and Y. Yamamoto, *J. Mater. Chem.*, 2003, **13**, 280.
20 A. C. Ferrari, J. C. Meyer, V. Scardaci, C. Casiraghi, M. Lazzeri, F. Mauri, S. Piscanec, D. Jiang, K. S. Novoselov, S. Roth and A. K. Geim, *Phys. Rev. Lett.*, 2006, **97**, 187401.
21 A. Reina, X. Jia, J. Ho, D. Nezich, H. Son, V. Bulovic, M. S. Dresselhaus and J. Kong, *Nano Lett.*, 2009, **9**, 30.
22 J. C. Meyer, A. K. Geim, M. I. Katsnelson, K. S. Novoselov, D. Obergfell, S. Roth, C. Girit and A. Zettl, *Solid State Commun.*, 2007, **143**, 101.
23 H. J. Park, J. Meyer, S. Roth and V. Skákalová, *Carbon*, 2010, **48**, 1088.
24 P. Y. Huang, C. S. Ruiz-Vargas, A. M. van der Zande, W. S. Whitney, M. P. Levendorf, J. W. Kevek, S. Garg, J. S. Alden, C. J. Hustedt, Y. Zhu, J. Park, P. L. McEuen and D. A. Muller, *Nature*, 2011, **469**, 389.
25 B. Guo, X. Wang, P. F. Fulvio, M. Chi, S. M. Mahurin, X. G. Sun and S. Dai, *Adv. Mater.*, 2011, **23**, 4661.
26 A. Yu, H. W. Park, A. Davies, D. C. Higgins, Z. Chen and X. Xiao, *J. Phys. Chem. Lett.*, 2011, **2**, 1855.
27 M. F. El-Kady, V. Strong, S. Dubin and R. B. Kaner, *Science*, 2012, **335**, 1326.